

PROBABILISTIC VALIDATION OF THE HOUSNER ROCKING MODEL

Jonas A. Bachmann^{1*}, Mathias Strand², Michalis F. Vassiliou¹, Marco
Broccardo¹, and Božidar Stojadinović¹

¹ETH Zürich
Stefano-Franscini-Platz 5, 8093 Zürich, Switzerland
{bachmann, vassiliou, stojadinovic}@ibk.baug.ethz.ch

²NTNU Trondheim
Høgskoleringen 1, 7491 Trondheim, Norway
mathias0strand@gmail.com

Keywords: Rocking, uplifting structures, earthquake engineering, chaotic motion, probabilistic analysis.

Abstract. *The rocking oscillator has drawn the attention of many researchers since the publication of Housner's [1] seminal paper. As the response of the rocking oscillator is highly non-linear and exhibits negative stiffness [2] many researchers have suggested treating the rocking oscillator as a chaotic system, in the sense that small perturbations of its governing parameters result to widely diverging outcomes. Researchers that have tried to experimentally validate Housner's model have shown that, given the modelling uncertainty, it is hard to confidently predict the time history response of a rocking block to a specific ground motion. This makes practicing engineers hesitant to adopt rocking as an earthquake response modification strategy.*

However, accurately predicting the response to a single ground motion would be ideal but it is not a necessary condition to trust a model: there is so much uncertainty in the expected ground motion that could overshadow the modelling uncertainty. To take the former uncertainty into account, in common practice, engineers use an ensemble of ground motions when they perform a time history analysis. Therefore, it is reasonable to try to compare numerical experimental testing results in terms of their statistics. If the numerical model is capable of capturing the statistics of the experimental testing, then, in terms of civil engineering design, the model is trustworthy. The first ones to adopt a probabilistic approach were Yim, Chopra and Penzien [3] who as early as in 1980 observed some order in rocking motion when they studied it from a probabilistic point of view. They observed specific trends in their numerical results when, instead of using only one, they used 10 synthetic ground motions. This paper compares the numerical and experimental response of a rigid rocking block when excited by an ensemble of 100 ground motions that share the statistical properties of original ground motion.

1 INTRODUCTION

The rocking oscillator has drawn the attention of many researchers since the publication of Housner's [1] seminal paper. Rocking behavior has been studied to address three classes of structures:

- a) large structures with underdesigned foundations that use uplift and rocking as a seismic response modification technique [4–15];
- b) precious unanchored equipment and museum artifacts that are excited by earthquakes and whose overturning stability is important [16,17]; and
- c) ancient Greek and Roman temples [18,19].

As the response of the rocking oscillator is highly non-linear, due to its negative stiffness [2], many have suggested treating the rocking oscillator as a chaotic system, in the sense that small perturbations of its governing parameters, be it the oscillator properties or the excitation, result to widely diverging outcomes. Researchers that have tried to experimentally validate Housner's model [20–26] have shown that, given the modelling uncertainty (especially of the one related to impact), it is difficult to confidently predict the time history response of a rocking block to a specific ground motion. Even if the coefficient of restitution is relatively well predicted, or determined via experiments, the response of the system to a ground motion is so sensitive that predicting the whole time history is practically impossible [27]. This has generated a lot of discussion about Housner's approach to determine the energy losses during impact and has resulted in various different energy dissipation models [28–37]. Moreover, it makes practicing engineers hesitant to adopt rocking as an earthquake response modification strategy, e.g. for bridges [8]. In contrast, Time History Analysis of yielding structures, where one has to model behaviors such as concrete cracking and spalling, rebar debonding or steel column buckling and connection failure, is accepted in engineering practice – even though research and "blind contests" show that predicting the response even of simple yielding structures is very sensitive to modelling assumptions [38] and that matching the experimental results is an extremely difficult task.

However, accurately predicting the response to a single ground motion would be ideal but it is not a necessary condition to trust a model (and the design solution it attempts to model): there is so much uncertainty in the expected ground motion that could overshadow the modelling uncertainty. In the cases where time history analyses are performed engineers commonly use an ensemble of ground motions to take the former uncertainty into account. Therefore, it is reasonable to try to compare numerical and experimental testing results in terms of their statistics. If the numerical model is capable of capturing the statistics of the experimental testing, then, regarding civil engineering design, the model is trustworthy. The first ones to adopt a probabilistic approach were Yim, Chopra and Penzien [3] who as early as in 1980 observed some order in rocking motion when they studied it from a probabilistic point of view. When, instead of using only one, they used 10 synthetic ground motions they observed specific trends in their numerical results. This shows that an order does exist in rocking motion.

This paper compares the statistics of the numerical and experimental response of a rigid rocking block when excited by an ensemble of 100 ground motions that have the similar spectral properties.

2 EMPLOYED NUMERICAL MODEL

The numerical model used in this study was kept as simple as possible, being the rigid rocking block on a rigid surface (Figure 1). It is assumed that the coefficient of friction is large enough to prevent sliding throughout the entire motion. The size and shape of the block are given by its semi-diagonal R , and its slenderness α , defined as $\alpha = \arctan(B/H)$. When the block is subjected to a horizontal ground acceleration $\ddot{u}_g(t)$, and is rocking around O, or O' respectively, the non-linear equation of motion is ([3, 39–41] among others):

$$I_0 \ddot{\theta}(t) + m_c g R [\alpha \operatorname{sgn} \theta(t) - \theta(t)] = -m_c \ddot{u}_g(t) R \cos[\alpha \operatorname{sgn} \theta(t) - \theta(t)] \quad (1)$$

Equation 1 can be expressed in a more compact form:

$$\ddot{\theta}(t) = -p^2 \left(\sin[\alpha \operatorname{sgn} \theta(t) - \theta(t)] + \frac{\ddot{u}_g}{g} \cos[\alpha \operatorname{sgn} \theta(t) - \theta(t)] \right) \quad (2)$$

where p is the frequency parameter defined as:

$$p = \sqrt{\frac{m_c g R}{I_0}} \quad (3)$$

To initiate rocking motion the ground acceleration \ddot{u}_g must meet or exceed the value $g \tan \alpha$. For rectangular blocks the rotational inertia is $I_0 = 4/3 m_c R^2$, and p simplifies to $p = \sqrt{(3g)/(4R)}$. The oscillation frequency T of a rigid block under free vibration is not constant because it strongly depends on the vibration amplitude θ_0 [1]. Nevertheless, the quantity p is a measure of the dynamic characteristics of the block and is equal to the in-plane pendulum frequency of the block as if it were hanging from its rocking rotation point [42]. For a free-standing solid rectangular block with dimensions $10m \cdot 1.5m$ the frequency parameter yields $p = 1.2 \text{ rad/s}$.

Housner assumed that the impact is instantaneous and that the impact forces are concentrated at the new pivot point (O and O'). Under these assumptions, Conservation

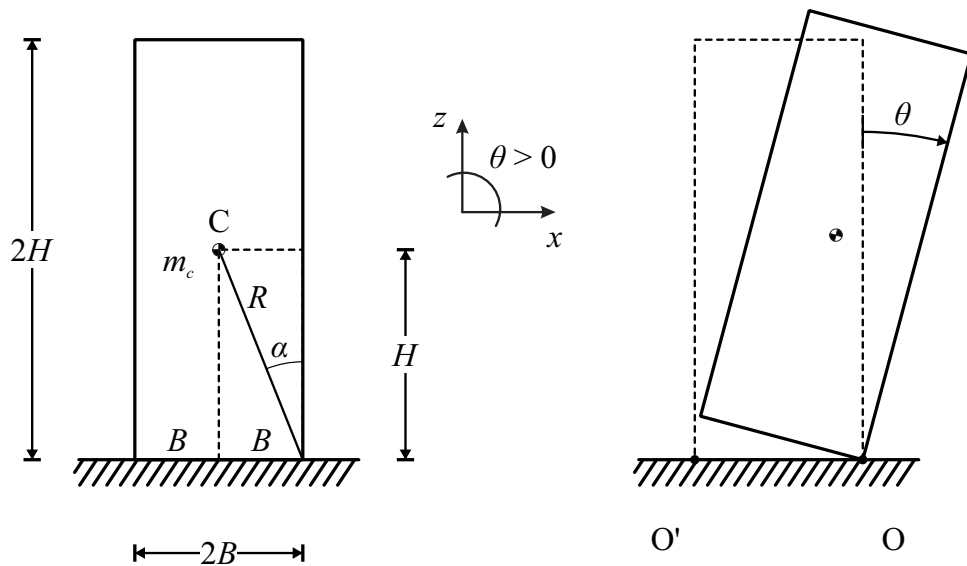


Figure 1: Rigid block rocking freely on a rigid surface.

of Angular Momentum (CoAM) an instant before the impact and immediately after the impact gives the coefficient of restitution:

$$r = \left(1 - 2 \sin^2 \alpha \frac{m_c R^2}{I_0}\right)^2 \quad (4)$$

Many researchers have revisited the above assumption [23, 25, 35, 43–45] and formulated more detailed expressions. In this study the Housner coefficient of restitution will be used due to the following:

- i. the specimens used were engineered such that impact forces act as close as possible to the rocking corners.
- ii. the Housner model is simple, and successful in identifying the most important energy dissipation factor: the slenderness α of the block.

The construction of the so called rocking spectra and the application of dimensional analysis to reduce the dimensionality of the problem are extensively described in [46–49], but are briefly described here for reasons of completeness: When excited by an analytical pulse ground motion [50] of a specific shape, a given acceleration amplitude a_p , and dominant frequency ω_p , the response θ of a rigid block is a function of five variables:

$$\theta = f(\alpha, R, g, a_p, \omega_p) \quad (5)$$

Since this function involves two reference dimensions ($[Length]$ and $[Time]$) it can be described by three dimensionless terms using Dimensional and Orientational Analysis [46–49] arguments:

$$\frac{\theta}{\alpha} = \phi\left(\alpha, \frac{\omega_p}{p}, \frac{a_p}{g \tan \alpha}\right) \quad (6)$$

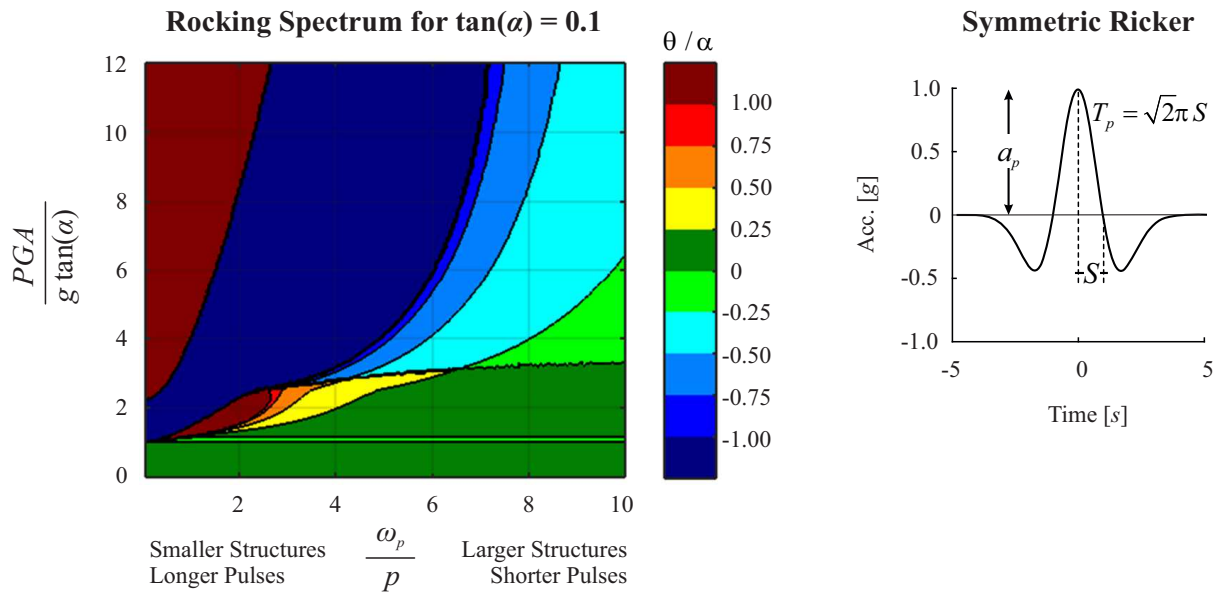


Figure 2: Rocking Spectrum (left) of a symmetric Ricker (right) analytical pulse ground motion.

Accordingly, rocking spectra (i.e. contour plots of θ/α in the ω_p/p and $a_p/g \tan \alpha$ plane for a given slenderness α can be constructed. Figure 2 plots such a spectrum for $\tan \alpha = 0.1$. One can observe that for small structures or long period pulses (small ω_p/p) the difference between the acceleration required to cause uplift ($\ddot{u}_g \geq g \tan \alpha$) and the acceleration required to overturn the block, is small. On the contrary, a larger structure (large ω_p/p) has a larger range of pulse accelerations for which there is rocking but no overturning. It is for these structures that the study of rocking motion is meaningful, whereas for small structures a simple static analysis is enough.

An acceleration equal to $g \tan \alpha$ is enough to cause both uplift and overturn. Therefore, this paper is limited to the study of relatively large (in the prototype scale) rocking structures.

3 SPECIMENS AND TEST SETUP

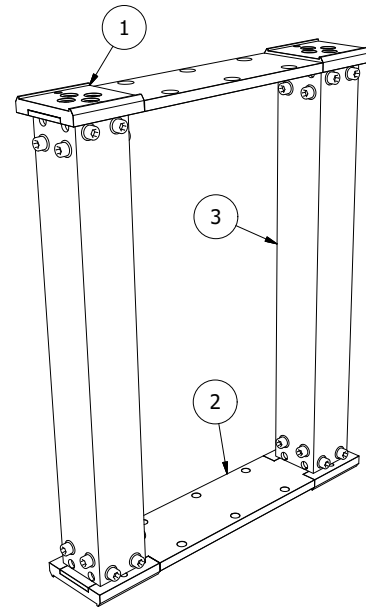
3.1 Rocking Specimen

With reference to Figure 3, a specimen consists of an assembly of four wedges (Nr. 1), two linking plates (Nr. 2), and two hollow columns (Nr. 3). It presents symmetry with respect to three planes. All parts are made of aluminum and connected by aluminum bolts. The specimen's height ($\equiv 2H$) is 500mm and its depth is 400mm . This specific depth of the specimen was chosen in order to avoid undesired out-of-plane motion. Previous tests using a specimen with equal width and depth revealed that, even for a weak 1D excitation, out-of-plane motion cannot be avoided.

The wedges used for the results presented in this manuscript had a total width of 82mm , but the effective rocking width (distance between the center of rotations O and O' while rocking occurs) was 75mm resulting in an effective slenderness of $\tan \alpha = 75\text{mm}/500\text{mm} = 0.15$. To represent as closely as possible the Housner impact model



(a) Specimen in ETH laboratory



(b) 3D model

Figure 3: Top: Specimen and 3D model

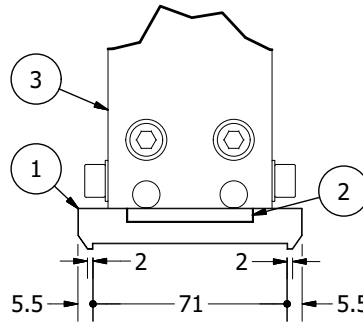


Figure 4: Close-up of wedges (units $[mm]$)

the center section of the wedges were carved out, leaving only a contact width of $2mm$ on each side (Figure 4). The setup was screwed together to allow for changes or replacements of specific parts while keeping the setup as simple as possible. The rocking column as shown in Figure 3a had a total weight of $3.94kg$. The natural eigenfrequency of the specimen was measured at $25Hz$ (corresponds to an eigenperiod of $0.04s$).

Recent research has questioned the Housner assumption regarding the point of action of the impact forces by either trying to determine the exact point of action of the impact forces [35] or by treating the location of the impact forces as a random variable [37]. The model examined herein does not focus on this problem which regards specimens with flat base. It represents structures that are designed to rock and their contact surfaces are designed such that the impact forces are concentrated as close to the corner as possible, in an effort both to increase damping and to decrease the uncertainty concerning the position of the impact forces. It has been shown [27] that, even if the impact forces are forced by design to act as close to the corner as possible, and even if this results to an excellent prediction of the coefficient of restitution, the rocking problem is so sensitive that it is impossible to predict the entire time history response. Thus, the need for probabilistic treatment arises.

3.2 Frequency Parameter and Coefficient of Restitution

In order to calibrate and validate the governing model parameters listed below, free vibration tests were performed in the ETH laboratory before the dynamic tests were executed.

- i. frequency parameter p , defined by equation (3)
- ii. coefficient of restitution r , defined by equation (4)

The frequency parameter p takes into account size R and rotational inertia I_0 and is therefore difficult to numerically accurately predict given the unequally distributed mass within the specimen, e.g. screws and bolts, linking plates etc. Therefore, p was solely

$p_{calibrated}$	$r_{calibrated}$	$r_{Housner}$	$\frac{r_{calibrated} - r_{Housner}}{r_{calibrated}}$
$4.8883s^{-1}$	0.9532	0.9465	0.70%

Table 1: Calibrated and theoretical properties of the rocking specimen

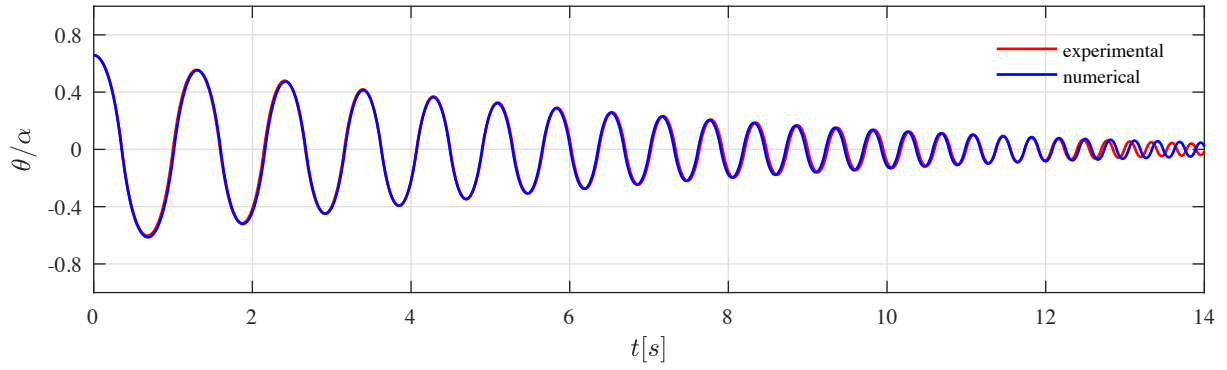


Figure 5: Free vibration: comparison between numerical ($p_{calibrated}$ and $r_{calibrated}$) and experimental data.

obtained from the laboratory and not compared to a computed numerical value. p was calibrated as $4.8883s^{-1}$ using the non-linear relationship between the rocking period T and the frequency parameter p was used [1]:

$$\cosh \frac{pT}{4} = \frac{1}{1 - \theta_0/\alpha} \quad (7)$$

where θ_0 is the maximum rocking angle for the half-cycle of duration $T/2$ (\equiv time between two impacts). For every half-cycle i a corresponding value p_i can be determined. The resulting values for p of the first 15 half-cycles were averaged to get $p_{calibrated}$. The influence of decreasing values for θ_0 over time was accounted for empirically by a regression performed on numerical experiments.

The experimental coefficient of restitution was derived by relating total energies pre- and post-impact to compute the energy loss at every impact, given the assumptions that energy dissipation only takes place during impact, and that at rest ($\theta = 0$) the potential energy is zero. The maximum angle $\theta_{0,i}$ of each half-cycle i was used to compute the corresponding increase of potential energy ΔV_i , at which point the angular velocity $\dot{\theta}$ is zero and, thus, the potential energy is equal to the total energy.

Eventually, equation (8) describes the energy loss at impact i and, therefore, the coefficient of restitution c_i for the i^{th} impact during a free vibration test.

$$c_i = \frac{\cos(\alpha - |\theta_{0,i+1}|) - \cos \alpha}{\cos(\alpha - |\theta_{0,i}|) - \cos \alpha} \quad (8)$$

Figure 5 plots the numerical and experimental outcome of the free vibration test after calibration ($p_{calibrated}$ was used), and Table 1 compares the calibrated parameter value for c to the one predicted by applying Housner's assumptions. Noticeably, the two time histories compare well for more than 20 rocking cycles. Housner's assumption predicts the coefficient of restitution with an error $< 1\%$ and the free vibration response is captured excellently. However, as it will be shown in a next section, this does not suffice to predict the complete time history response to a ground motion.

3.3 Specimen Excitation and Shaking Table

The rocking response of the specimen was induced by dynamic excitation of its support. This was achieved by placing the specimen on the top of the ETH shaking table [51]. The

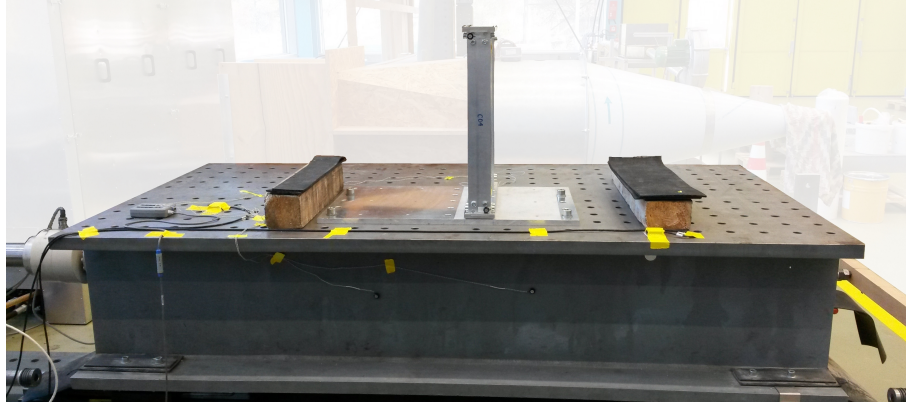


Figure 6: Experimental setup on the shaking table

shaking table platform is a stiff steel box that is placed on roller bearings and actuated using a servo-hydraulic actuator to move only in a uniaxial, horizontal direction. The stroke of the table is 250mm and the maximum velocity is 225mm/s .

3.4 Data Acquisition System

Figure 6 shows the experimental and Figure 7 the schematic setup on the shaking table. The movement of the rocking column during the experimental tests was tracked with the Optotrak Certus System, manufactured by Northern Digital Inc. (NDI). In total four infrared-emitting diodes were placed as markers numbered from 1 to 4; two of them on the rocking specimen (Nr. 2 and 4), and two on the shaking table (Nr. 1 and 3). The markers recorded 3D position data with an accuracy of 0.1mm . Additional output, recorded with the same sampling rate of 500Hz , is the 2D-angle (in the plane $x - y$ of the NDI coordinate system) between the two lines 1–3 (going through the markers Nr. 1 and 3) and 2–4, respectively, and is computed by the software of the NDI system.

In the given configuration, respecting the feasible measurement window while allowing the shaking table to move to its maximum positions, the NDI camera allowed for recording angles with an error of 0.8mrad ($= 0.0053\alpha$). The initial and constant offset between the

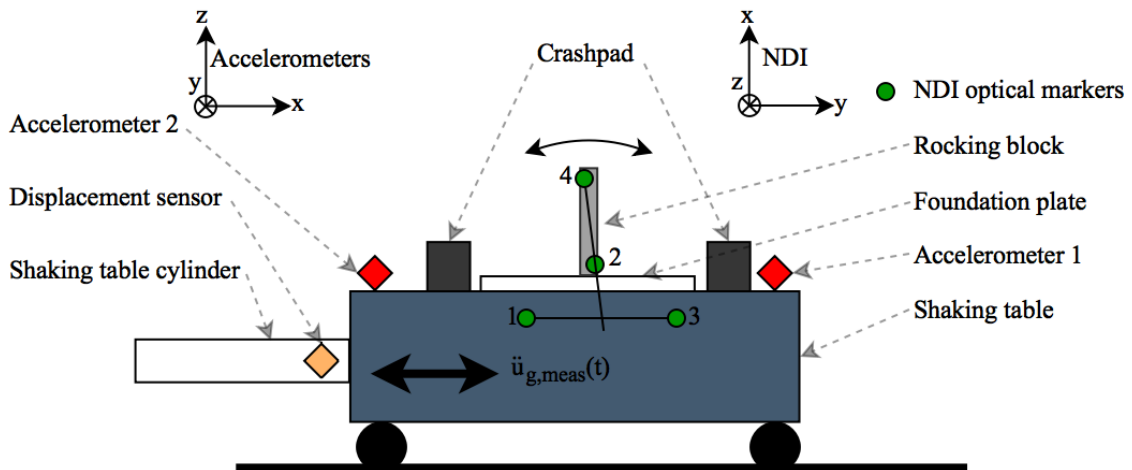


Figure 7: Schematic setup on the shaking table

Lines 1–3 and 2–4 was measured at rest (no rocking) and was subtracted during post processing. The NDI camera was positioned such that the y-axis of the NDI camera and the moving 1D-axis of the shaking table were parallel. Post processing of the 3D position data showed that this alignment was flawless.

4 DESCRIPTION OF THE SYNTHETIC GROUND MOTION GENERATION MODEL

In their pioneering work in 1980 Yim, Chopra and Penzien [3] used the 1968 model of Jennings *et al.* [52] to generate synthetic ground motions. Since then, more sophisticated models have been developed that produce simulated ground motions with similar elastic spectra characteristics to a given recorded ground motion. The Rezaeian and Der Kiureghian [53–55] stochastic ground motion model was used to create 100 synthetic ground motions for the longitudinal component of the 1940 El Centro Array #9 earthquake.

The set of 100 synthetic ground motion records was created such that it statistically matches the original motion. Figure 8a),b) shows the acceleration trace of the original ground motion as well as the elastic pseudo-acceleration response spectra of the generated

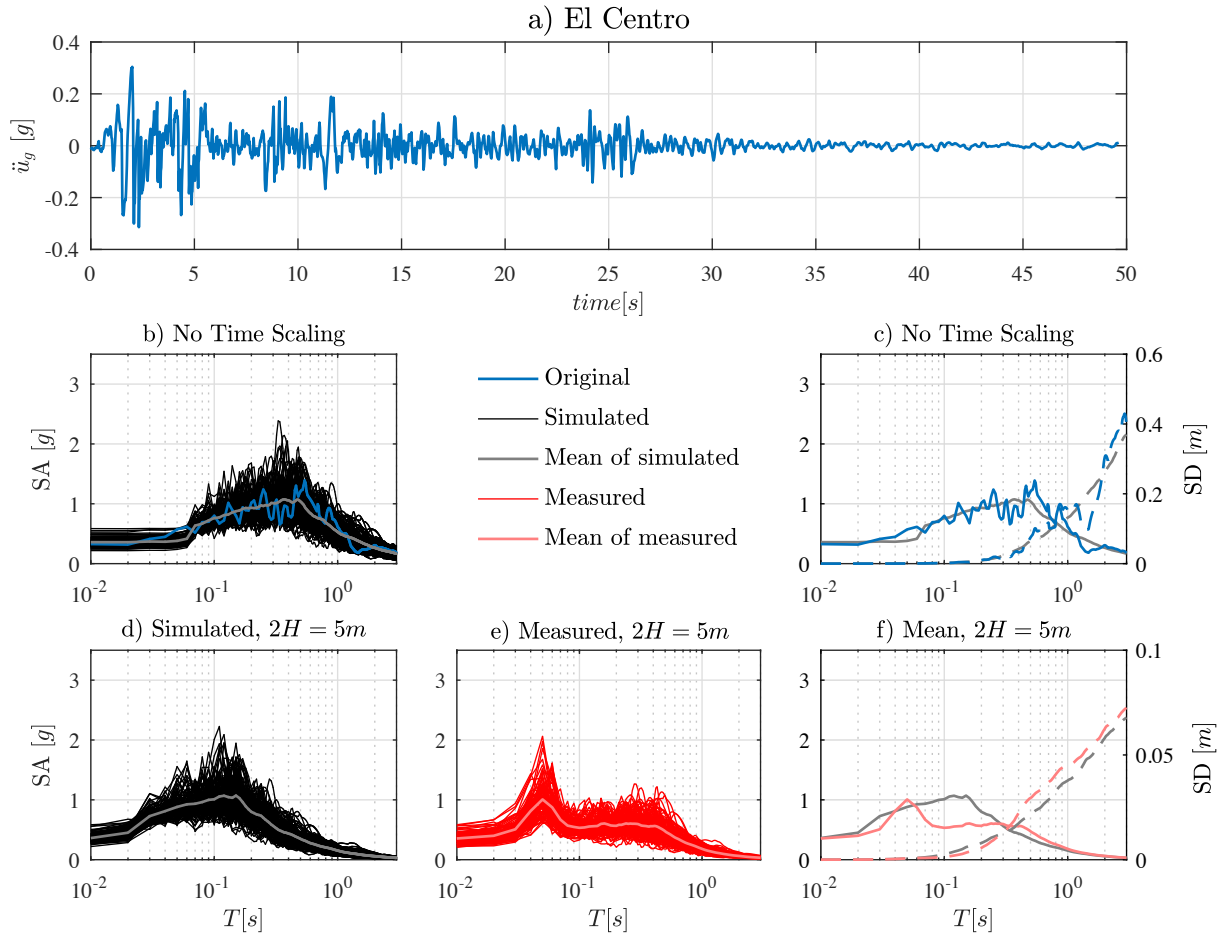


Figure 8: a) El Centro ground motion; b) Acceleration spectra of the recorded and the simulated ground motion (without time scaling); c) Mean acceleration and displacement spectra of the original and simulated ground motions d-f) Acceleration and displacement spectra of the simulated ground motions and their shake table realizations (with time scaling).

synthetic ground motion records.

Note that the simulated ground motions merely match the original ground motion in terms of selected response quantities of a linear elastic single-degree-of-freedom oscillator. This does not guarantee that structures with non-linear behavior, such as rocking structures, will have similar responses to individual ground motions in the generated ensemble. In fact, Vassiliou *et al.* [56] have shown that ground motions with identical elastic spectra can have very different rocking spectra. However, as there is no stochastic model to generate ground motions with same overturning potential, using ground motions with similar elastic spectra was adopted as a minimum precondition for the statistical comparison of the numerical and experimental results.

It is expected that the predictability of rocking motion will depend on the size of the rocking structure. From equation (6) it follows directly that to study this dependency, instead of using different specimens, one can change the time scale of the ground motion. Therefore, the dominant frequency of the input ground motions in the model scale will be:

$$\omega_{model} = \omega_{prototype} \sqrt{S} \quad (9)$$

where S is the size scaling factor ($S = R_{prototype}/R_{model}$).

The prototype column that was tested had a total height $2H$ equal to $5m$. Given that in the model domain the size of the specimen is $0.5m$, the ground motions were scaled in time by a factor of $\sqrt{10}$ (i.e. their dominant frequency was increased). Note that the 100 simulated ground motions were produced in the prototype scale and afterwards they were scaled in time; not the vice versa.

Figure 8 compares the elastic spectra of the 100 simulated ground motions both in the prototype scale and when the ground motions are scaled in time. The spectra of both the simulated time histories (i.e. the input to the shaking table) and of the measured shaking table motion are shown. The mean of the displacement spectra of the 100 motions is also plot, as several researchers report that the maximum of the Elastic Displacement Spectrum is a good measure of the overturning potential of a ground motion [57–59].

One can observe that Rezeian’s and Der Kiureghian’s model succeeds in producing synthetic ground motions with similar elastic spectra to the recorded ones. A comparison between the spectra of the simulated ground motions and of the spectra of the motions measured on the shaking table shows that the shaking table generally failed to reproduce well the high frequency content of the input ground motions. However, this does not jeopardize the validity of the comparison between the response predicted by the numerical rocking model and the experimentally observed rocking response: The spectra of the *measured* ground motion still do not have a large dispersion. In any case, the numerical model uses the measured acceleration as excitation; and *not* the input to the shaking table controller.

5 DETERMINISTIC COMPARISON

Figure 9 shows the responses observed experimentally and determined numerically for the prototype model size of $5m$ to four randomly selected synthetic ground motions (out of the set of 100) of the original ground motion Lefkada. It demonstrates that, even though the experimentally measured frequency parameter, p , was used, Housner’s model fails to

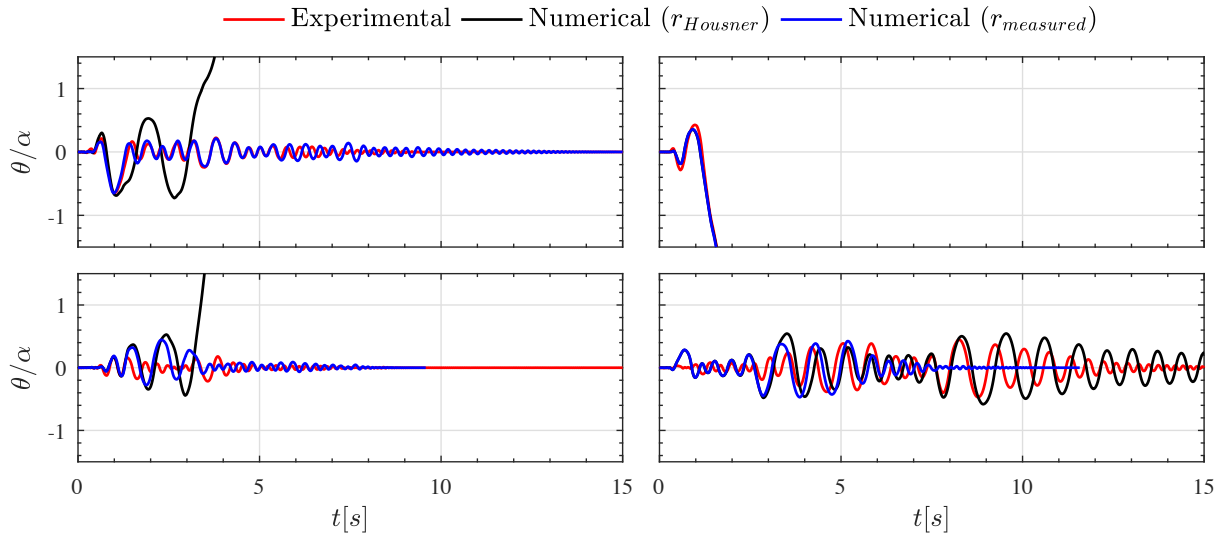


Figure 9: Deterministic comparison of time history responses to four randomly selected simulated ground motion: experimental vs. numerical (Housner) vs. numerical (empirical).

predict the response well. The results improve when the experimentally obtained coefficient of restitution is used. Nevertheless, the prediction in most cases is poor and there is not a consistent overestimation or underestimation of the maximum rocking response. Similarly, this can be observed in the other produced synthetic ground motions.

It can be concluded that the Housner rocking model, even when the coefficient of restitution is experimentally obtained with free vibration tests, is unable to confidently predict the response to a recorded earthquake ground motion. In an effort to estimate whether the model can predict the statistics of the response to an ensemble of ground motions (which is the actual design question) the next section adopts a probabilistic treatment.

6 STATISTICAL COMAPRISON

The experimental and the numerical response are compared in terms of their maximum rotation because this is the engineering parameter that is of interest to the designer.

Next, following [3] the maxima of θ/α were arranged in ascending order and plotted in Figure 10 in the form of a cumulative probability distribution function (CDF). This plot shows the probability that the block will exhibit a response less than a specific value

	θ_{num}	θ_{exp}	$\theta_{num} - \theta_{exp}$	$\frac{\theta_{num} - \theta_{exp}}{\theta_{exp}}$
percentile	$[\alpha]$	$[\alpha]$	$[\alpha]$	$[-]$
25 th	0.37	0.36	0.01	0.03
50 th	0.77	0.65	0.12	0.18
75 th	overturn	overturn	-	-

Table 2: 25th, 50th and 75th percentile of the responses to the El Centro ground motion for the 5m tall prototype.

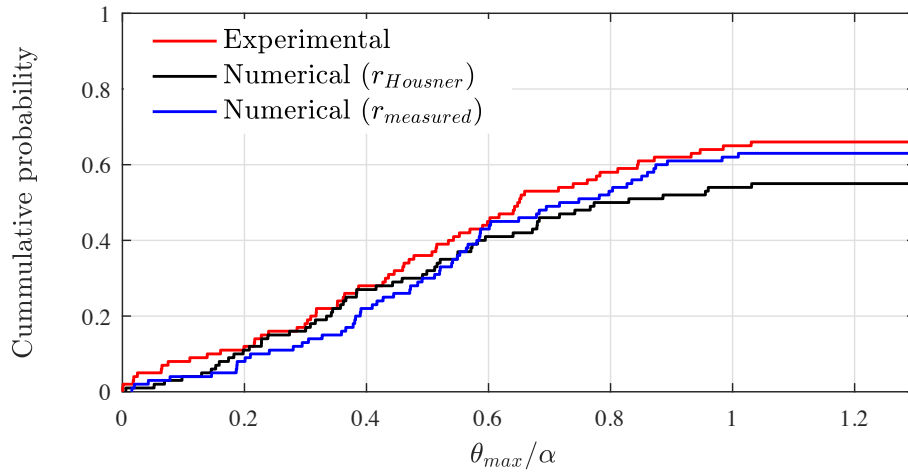


Figure 10: Cumulative distribution functions (CDF) of maximum tilt angle θ_{max} normalized by slenderness α .

of θ/α . Table 2 shows that the numerical and the experimental models compare excellent in terms of the 25th, 50th and 75th percentile of θ/α with a maximum relative error of 0.18. This is considered a good prediction, especially given the uncertainty in predicting the level of the ground motion intensity (however it is defined).

A comparison between the probabilities of overturning when the Housner coefficient of restitution and when the empirical coefficient of restitution are used reconfirms the 1980 finding of Yim *et al.* [3]:

"From a probabilistic point of view, the coefficient of restitution influences the response [...] to a much lesser degree than the other system parameters."

Therefore, for blocks with bases engineered to attract all the impact forces at the corners, it seems pointless (at least in terms of overturning probability) to try to revisit the coefficient of restitution proposed by Housner via sophisticated models. On the contrary, it is more useful to evaluate the stability of a rocking block probabilistically via the use of an ensemble of ground motions.

CONCLUSIONS

The rocking response to a single ground motion is indeed very sensitive to all parameters and the prediction of the response of a rocking block to a single ground motion is a very difficult task. In that sense, it could be characterized as "chaotic". However, since the seismic problem is inherently stochastic (the ground motion is not known a priori and this induces uncertainty in the system), the modelling uncertainty should not be a reason to deter engineers from using rocking solutions. This paper compared experimental and numerical results of planar SDOF rocking. It showed that existing rigid rocking models are able to predict the statistics of the behavior of rigid rocking systems with an accuracy on the order of 18%, at least when their rocking surfaces are engineered in a way so that the impact forces are concentrated at the edges.

REFERENCES

- [1] G.W. Housner. The Behavior of inverted Pendulum Structures during Earthquakes. *Bulletin of the Seismological Society of America*, 53(2):403–417, 1963.
- [2] Nicos Makris and Dimitrios Konstantinidis. The rocking spectrum and the limitations of practical design methodologies. *Earthquake Engineering & Structural Dynamics*, 32(2):265–289, feb 2003.
- [3] Chik-Sing Yim, Anil K. Chopra, and Joseph Penzien. Rocking response of rigid blocks to earthquakes. *Earthquake Engineering & Structural Dynamics*, 8(6):565–587, 1980.
- [4] John B Mander and Chin-Tung Cheng. Seismic resistance of bridge piers based on damage avoidance design. Technical report, 1997.
- [5] Junichi Sakai and Stephen A Mahin. *Analytical investigations of new methods for reducing residual displacements of reinforced concrete bridge columns*. Pacific Earthquake Engineering Research Center, 2004.
- [6] Chin-Tung Cheng. Shaking table tests of a self-centering designed bridge substructure. *Engineering Structures*, 30(12):3426–3433, 2008.
- [7] Michalis F. Vassiliou. *Analytical investigation of the dynamic response of a pair of columns capped with a rigid beam and of the effect of seismic isolation on rocking structures*. PhD thesis, Doctoral dissertation, Dept. of Civil Engineering, Univ. of Patras, Greece (in Greek), 2010.
- [8] Lijun Deng, Bruce L Kutter, and Sashi K Kunnath. Probabilistic seismic performance of rocking-foundation and hinging-column bridges. *Earthquake Spectra*, 28(4):1423–1446, 2012.
- [9] Nicos Makris and Michalis F. Vassiliou. Planar rocking response and stability analysis of an array of free-standing columns capped with a freely supported rigid beam. *Earthquake Engineering & Structural Dynamics*, 42(3):431–449, mar 2013.
- [10] Nicos Makris and Michalis F. Vassiliou. Are Some Top-Heavy Structures More Stable? *Journal of Structural Engineering*, 140(5):06014001, may 2014.
- [11] Nicos Makris and Michalis F. Vassiliou. Dynamics of the Rocking Frame with Vertical Restraints. *Journal of Structural Engineering*, 141(10):04014245, oct 2015.
- [12] Elias G. Dimitrakopoulos and Anastasios I Giouvanidis. Seismic Response Analysis of the Planar Rocking Frame. *Journal of Engineering Mechanics*, 141(7):04015003, jul 2015.
- [13] Anastasios I. Giouvanidis and Elias G. Dimitrakopoulos. Seismic Performance of Rocking Frames with Flag-Shaped Hysteretic Behavior. *Journal of Engineering Mechanics*, (accepted 5 OCT), 2016.
- [14] Marianna Loli, Jonathan A Knappett, Michael J Brown, Ioannis Anastasopoulos, and George Gazetas. Centrifuge modeling of rocking-isolated inelastic RC bridge piers. *Earthquake engineering & structural dynamics*, 43(15):2341–2359, 2014.
- [15] P. Kokkali, T. Abdoun, and I. Anastasopoulos. Centrifuge Modeling of Rocking Foundations on Improved Soil. *Journal of Geotechnical and Geoenvironmental Engineering*, 141(10):4015041, 2015.
- [16] Amitabh Dar, Dimitrios Konstantinidis, and Wael W. El-Dakhakhni. Evaluation of ASCE 43-05 Seismic Design Criteria for Rocking Objects in Nuclear Facilities. *Journal of Structural Engineering*, page 04016110, jun 2016.
- [17] Alessandro Contento and Angelo Di Egidio. Investigations into the benefits of base isolation for non-symmetric rigid blocks. *Earthquake Engineering & Structural Dynamics*, 38(7):849–866, jun 2009.

- [18] Ioannis N. Psycharis, J. V. Lemos, D. Y. Papastamatiou, C. Zambas, and C. Papantonopoulos. Numerical study of the seismic behaviour of a part of the Parthenon Pronaos. *Earthquake Engineering & Structural Dynamics*, 32(13):2063–2084, nov 2003.
- [19] Dimitrios Konstantinidis and Nicos Makris. Seismic response analysis of multidrum classical columns. *Earthquake Engineering & Structural Dynamics*, 34(10):1243–1270, aug 2005.
- [20] MJN Priestley, RJ Evison, and AJ Carr. Seismic response of structures free to rock on their foundations. *Bulletin of the New Zealand National*, 1978.
- [21] Mohammad Aslam, D Theodore Scalise, and William G Godden. Earthquake rocking response of rigid bodies. *Journal of the Structural Division*, 106(2):377–392, 1980.
- [22] P. R. Lipscombe and S. Pellegrino. Free Rocking of Prismatic Blocks. *Journal of Engineering Mechanics*, 119(7):1387–1410, jul 1993.
- [23] Fernando Peña, Francisco Prieto, Paulo B. Lourenço, A. Campos Costa, and J. V. Lemos. On the dynamics of rocking motion of single rigid-block structures. *Earthquake Engineering & Structural Dynamics*, 36(15):2383–2399, dec 2007.
- [24] Quincy Tsun Ming Ma. *The mechanics of rocking structures subjected to ground motion*. PhD thesis, 2010.
- [25] Rico E. Truniger, Michalis F. Vassiliou, and Božidar Stojadinović. An analytical model of a deformable cantilever structure rocking on a rigid surface: experimental validation. *Earthquake Engineering & Structural Dynamics*, 44(13), 2015.
- [26] Rico E. Truniger, Michalis F. Vassiliou, and Božidar Stojadinović. Experimental Study on the Interaction between Elasticity and Rocking. In *10th U.S. National Conference on Earthquake Engineering*, 2014.
- [27] Jonas A. Bachmann, Christoph Jost, Quentin Studemann, Michalis F. Vassiliou, and Božidar Stojadinovic. An analytical model for the dynamic response of an elastic SDOF system fixed on top of a rocking single-story frame structure: experimental validation. In *EC-COMAS Congress 2016: 7th European Congress on Computational Methods in Applied Sciences and Engineering*, Heraklion, 2016.
- [28] Giuseppe Oliveto, Ivo Calì, and Annalisa Greco. Large displacement behaviour of a structural model with foundation uplift under impulsive and earthquake excitations. *Earthquake Engineering & Structural Dynamics*, 32(3):369–393, mar 2003.
- [29] F. Prieto, P. B. Lourenço, and C. S. Oliveira. Impulsive Dirac-delta forces in the rocking motion. *Earthquake Engineering & Structural Dynamics*, 33(7):839–857, jun 2004.
- [30] Sinan Acikgoz and Matthew J. DeJong. The interaction of elasticity and rocking in flexible structures allowed to uplift. *Earthquake Engineering & Structural Dynamics*, 41(11):1–18, mar 2012.
- [31] Alessandro Baratta, Ileana Corbi, and Ottavia Corbi. Towards a seismic worst scenario approach for rocking systems: analytical and experimental set-up for dynamic response. *Acta Mechanica*, 224(4):691, 2013.
- [32] Michalis F. Vassiliou, Rico E. Truniger, and Božidar Stojadinović. An analytical model of a deformable cantilever structure rocking on a rigid surface: development and verification. *Earthquake Engineering & Structural Dynamics*, 44(13), 2015.
- [33] Sinan Acikgoz and Matthew J. DeJong. Analytical modelling of multi-mass flexible rocking structures. *Earthquake Engineering & Structural Dynamics*, 41(11):1549–1568, 2016.
- [34] Anastasios I. Giouvanidis and Elias G. Dimitrakopoulos. Nonsmooth Dynamic Analysis of Sticking Impacts in Rocking Structures. *Bulletin of Earthquake Engineering*, (accepted 4 DEC), 2016.

- [35] Dimitrios Kalliontzis, Sri Sritharan, and Arturo Schultz. Improved Coefficient of Restitution Estimation for Free Rocking Members. *Journal of Structural Engineering*, page 06016002, jul 2016.
- [36] Michalis F. Vassiliou, Kevin R. Mackie, and Božidar Stojadinović. A finite element model for seismic response analysis of deformable rocking frames. *Earthquake Engineering & Structural Dynamics*, 2016.
- [37] M N Chatzis, M Garcia Espinosa, and A W Smyth. Examining the Energy Loss in the Inverted Pendulum Model for Rocking Bodies. *Journal of Engineering Mechanics*, page 4017013, 2017.
- [38] V Terzic, M J Schoettler, J I Restrepo, and S A Mahin. Concrete column blind prediction contest 2010: outcomes and observations. *PEER Rep. No.*, 1, 2015.
- [39] Jian Zhang and Nicos Makris. Rocking Response of Free-Standing Blocks under Cycloidal Pulses. *Journal of Engineering Mechanics*, 127(5):473–483, may 2001.
- [40] Nicos Makris. The Role of the Rotational Inertia on the Seismic Resistance of Free-Standing Rocking Columns and Articulated Frames. *Bulletin of the Seismological Society of America*, 104(5):2226–2239, oct 2014.
- [41] Nicos Makris and Georgios Kampas. Size Versus Slenderness: Two Competing Parameters in the Seismic Stability of Free-Standing Rocking Columns. *Bulletin of the Seismological Society of America*, 106(1):104–122, feb 2016.
- [42] Elias G. Dimitrakopoulos and Matthew J. DeJong. Overturning of Retrofitted Rocking Structures under Pulse-Type Excitations. *Journal of Engineering Mechanics*, 138(8):963–972, aug 2012.
- [43] Mohamed A. ElGawady, Quincy Tsun Ming Ma, John W. Butterworth, and Jason Ingham. Effects of interface material on the performance of free rocking blocks. *Earthquake Engineering & Structural Dynamics*, 40(4):375–392, apr 2011.
- [44] Christine E. Wittich and Tara C. Hutchinson. Shake table tests of stiff, unattached, asymmetric structures. *Earthquake Engineering & Structural Dynamics*, 41(11):n/a–n/a, jun 2015.
- [45] Tamás Ther and László P Kollár. Refinement of Housner’s model on rocking blocks. *Bulletin of Earthquake Engineering*, pages 1–15.
- [46] Elias G. Dimitrakopoulos and Matthew J. DeJong. Revisiting the rocking block: closed-form solutions and similarity laws. *Proceedings of the Royal Society A: Mathematical, Physical and Engineering Sciences*, 468(2144):2294–2318, aug 2012.
- [47] Nicos Makris and Michalis F. Vassiliou. Sizing the slenderness of free-standing rocking columns to withstand earthquake shaking. *Archive of Applied Mechanics*, 82(10-11):1497–1511, oct 2012.
- [48] Michalis F. Vassiliou and Nicos Makris. Analysis of the rocking response of rigid blocks standing free on a seismically isolated base. *Earthquake Engineering & Structural Dynamics*, 41(2):177–196, feb 2012.
- [49] Michalis F. Vassiliou and Nicos Makris. Dynamics of the Vertically Restrained Rocking Column. *Journal of Engineering Mechanics*, 141(12):04015049, dec 2015.
- [50] Michalis F. Vassiliou and Nicos Makris. Estimating time scales and length scales in pulselike earthquake acceleration records with wavelet analysis. *Bulletin of the Seismological Society of America*, 101(2):596–618, 2011.
- [51] Hugo Bachmann, Thomas Wenk, Markus Baumann, and Pierino Lestuzzi. Der neue ETH-Erdbebensimulator. *Schweizer Ingenieur und Architekt*, 4, 1999.

- [52] Paul C Jennings, George W Housner, and N Chien Tsai. Simulated earthquake motions. 1968.
- [53] Sanaz Rezaeian and Armen Der Kiureghian. Simulation of synthetic ground motions for specified earthquake and site characteristics. *Earthquake Engineering & Structural Dynamics*, 39(10):1155–1180, 2010.
- [54] Sanaz Rezaeian and Armen Der Kiureghian. A stochastic ground motion model with separable temporal and spectral nonstationarities. *Earthquake Engineering & Structural Dynamics*, 37(13):1565–1584, 2008.
- [55] M Broccardo and A Der Kiureghian. Simulation of near-fault ground motions using frequency-domain discretization. In *Proceedings of the 10th National Conference on Earthquake Engineering. Anchorage, Alaska*, 2014.
- [56] Michalis F. Vassiliou, Stefan Burger, Marius Egger, Jonas A. Bachmann, Marco Broccardo, and Božidar Stojadinović. The three-dimensional behavior of inverted pendulum cylindrical structures during earthquakes (under review). *Earthquake Engineering & Structural Dynamics*.
- [57] Bidur Kafle, Nelson T. K. Lam, Emad F. Gad, and John Wilson. Displacement controlled rocking behaviour of rigid objects. *Earthquake Engineering & Structural Dynamics*, 40(15):1653–1669, dec 2011.
- [58] F. Gelagoti, R. Kourkoulis, I. Anastasopoulos, and G. Gazetas. Rocking-isolated frame structures: Margins of safety against toppling collapse and simplified design approach. *Soil Dynamics and Earthquake Engineering*, 32(1):87–102, jan 2012.
- [59] Vasileios Drosos and Ioannis Anastasopoulos. Shaking table testing of multidrum columns and portals. *Earthquake Engineering & Structural Dynamics*, 43(11):1703–1723, sep 2014.